Journal of Alloys and Compounds 489 (2010) 51–55

Contents lists available at ScienceDirect

Journal of Alloys and Compounds

journal homepage: www.elsevier.com/locate/jallcom

Review

Oriented growth of ZnO nanostructures on different substrates via a hydrothermal method

Jinghai Yang[a,*], Jiahong Zheng[a], Hongju Zhai[a], Xiangmin Yang[b], Lili Yang[a], Yang Liu[a], Jihui Lang[a], Ming Gao[a]

[a] The Institute of Condensed State Physics, Jilin Normal University, Siping 136000, China
[b] Training Center of Jilin Petrochemical Company, PetroChina, Jilin 132022, China

ARTICLE INFO

Article history:
Received 13 June 2009
Received in revised form 27 August 2009
Accepted 28 August 2009
Available online 23 September 2009

Keywords:
Nanostructures
X-ray diffraction microscopy
Optical properties

ABSTRACT

Well-oriented ZnO nanorod arrays are successfully fabricated on different substrates. They are formed on different substrates at low temperature via a hydrothermal method, without adding any catalysts or templates. This approach is convenient and inexpensive. The morphologies of ZnO crystals could be controlled and transformed to other morphologies successfully by using different substrates. The effects of the substrates on the ZnO nanorod arrays have been systematically studied by X-ray diffraction (XRD) and scanning electron microscopy (SEM). The characterizations of XRD and scanning electron microscopy (SEM) reveal that these products are pure single-crystal and the structure is uniform. The photoluminescence property has been detected by photoluminescence (PL) spectrum and Raman spectrum. Photoluminescence measurements show that each spectrum consists of the ultraviolet (UV) band and a relative broad visible light emission peak. But substrates play roles in the intensity of ultraviolet and visible light emission peak. The green emission in Raman measurement may be related to the surface states.

Published by Elsevier B.V.

Contents

1. Introduction

During the past few years, much attention has been focused on the research of quasi-one-dimensional nanostructured semiconductor materials, such as nanowires, nanorods and nanotubes, due to their novel physical and chemical properties and wide range of potential applications in nanodevices [1–10]. Zinc oxide (ZnO), a direct wide band gap (3.37 eV) semiconductor with a large excitation binding energy (60 meV), is one of the most important multifunctional oxide ceramic materials possessing a suite of useful properties, such as optical absorption and emission, piezoelectricity, transparent conductivity, high voltage–current nonlinearity, sensitivity to gases, and photocatalysis [11,12]. The research of highly oriented, aligned and ordered arrays ZnO nanorods attracts the worldwide interests. Because of their electrical and optical properties [13], ZnO nanopencils with a fine nanotip can be used in biosensors, which can greatly enhance the immobilization of DNA and protein molecules.

Gas-phase [14–18] and solution-phase [19–26] syntheses are the two main approaches adopted for the fabrication of ZnO nanostructures, in which, the hydrothermal method is more promising for fabricating ideal nanomaterial with special morphology due to the simple, fast, less expensive, low growth temperature, high yield and scalable process.

In recent years, most of the reports failed to produce ZnO nanorod arrays at relatively low temperature although many of them were on the preparation of 1D ZnO nanostructures via hydrothermal methods [27,28]. Moreover, little work has been

* Corresponding author. Tel.: +86 434 3294566; fax: +86 434 3294566.
E-mail address: jhyang1@jlnu.edu.cn (J. Yang).

0925-8388/$ – see front matter. Published by Elsevier B.V.
doi:10.1016/j.jallcom.2009.08.159

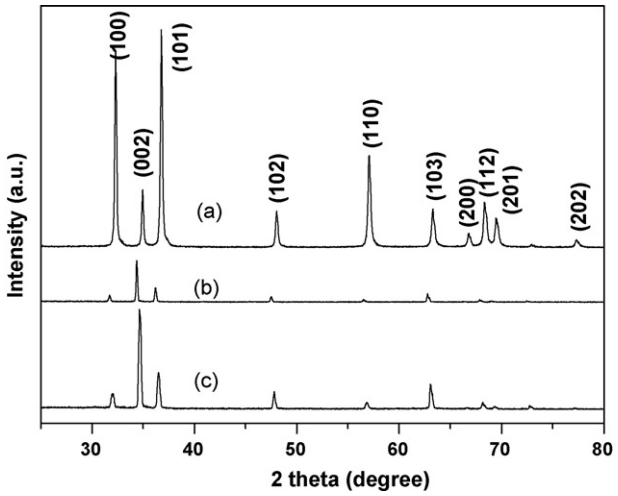

Fig. 1. XRD patterns of the as-prepared ZnO nanorods on different substrate of a bare Si substrate (a), Cu substrate (b) and Si substrate coated with ZnO seeds (c).

focused on the preparation of ZnO nanorod arrays by using different substrates, especially on the effects of the substrates on the morphologies and photoluminescence properties. Therefore, how to fabricate well aligned and oriented 1D ZnO nanorods on different substrates at low temperature with a low cost still remains a great challenge.

In this article, we reported the syntheses of the pencil-like and well aligned and oriented 1D ZnO nanorods via a hydrothermal method on different substrates at relatively low temperature. Water was used as the solvent without any catalysts or templates, because water was much cheaper and more environment friendly than alcohol. And the effects of different substrates on their structures, morphologies and photoluminescence properties were investigated in the article.

2. Experimental

All chemicals (analytical grade reagents) were purchased from Shenyang Chemical Reagents Company and used without further purification. The synthesis of ZnO nanorods was performed according to a hydrothermal reaction route with different substrates (Si, Cu and Si substrate coated with ZnO seeds by pulsed laser deposition (PLD)). A typical procedure was as follows: the ammonia (25%) was gradually added to the solution of zinc chloride ($ZnCl_2$, Aldrich, purity 98%, 0.1 M) to pH nearly to 10 with stirring. The mixed solution was transferred into four Teflon-lined stainless steel autoclaves with a capacity of 50 mL. Then, the bare Si wafer, the Cu substrate and the Si substrate coated with ZnO seeds were immersed into the reaction solution. Finally, sealing and heating the Teflon-lined stainless steel autoclave at 90 °C for 8 h in an ordinary laboratory oven. Subsequently, the autoclave was cooled to room temperature. After thoroughly washing several times with deionized water and drying at 60 °C under air atmosphere, a white layer of product was deposited on the substrates and kept for further characterization.

To characterize the ZnO products, X-ray power diffraction (XRD) experiments were performed on a D/max-RA XRD diffraction spectrometer with a Cu Kα line at 1.5406 Å. Scanning electron microscope (SEM) (Hitachi, S-570) measurements were also used to investigate the surface morphology of the samples. The optical properties were obtained by the photoluminescence (PL) measurements using HR800 LabRam Infinity Spectrophotometer excited by a continuous He–Cd laser with a wavelength of 325 nm at a power of 50 mW. Raman spectra were excited with the 514 nm line of an Ar^+ laser at an incident power of 20 mW.

3. Results and discussion

The XRD patterns (Fig. 1) of ZnO products with different substrates exhibit a point in common: for each sample, all the observed diffraction peaks can be indexed to a ZnO (JCPDS card, No. 80-0074) wurtzite structure, and no other impurity phase was found. Fig. 1(b) and (c) shows the XRD patterns of highly oriented ZnO nanorods grown on Cu substrate and Si substrate coated with ZnO seeds, respectively. In the XRD patterns, the position of peaks in sample (b) shifted to a lower angle compared with the other two samples was due to the lattice mismatch between ZnO nanorods and Cu substrate [29]. It is worthy of noticing that relative intensity of the (0 0 2) diffraction peak exists at 34.65° is much higher, compared with the standard XRD pattern, which further illustrates the substrate's effect on the highly preferential orientation of ZnO nanorod arrays along *c*-axis. It indicates that the ZnO nanorod arrays tend to grow perpendicular to the substrate surface. Furthermore, the relative intensities of these peaks are distinct from those of ZnO powders. The diffraction intensity of the (0 0 2) surpasses the others, which illustrates the *c*-oriented nature of the as grown array. The degree of the orientation can be illustrated by the relative texture coefficient [30], which is given by

$$TC_{0002} = \frac{I_{0002}/I^0_{0002}}{I_{0002}/I^0_{0002} + I_{10\bar{1}0}/I^0_{10\bar{1}0}}$$

where TC_{0002} is the relative texture coefficient of diffraction peaks (0 0 0 2) over (1 0 $\bar{1}$ 0), I_{0002} and $I_{10\bar{1}0}$ are the measured diffraction intensities due to (0 0 0 2) and (1 0 $\bar{1}$ 0) planes, respectively, and I_{0002} and $I_{10\bar{1}0}$ are the corresponding values of standard JCPDS card measured from randomly oriented powder samples. For materials with random crystallographic orientations, the texture coefficient is 0.5, while the value for our sample is 0.56, which shows a preferential orientation along the *c*-axis for the ZnO nanorod array.

Fig. 2 shows the SEM images of ZnO nanorod grown on the three kinds of substrates. From Fig. 2(a), the panoramic view reveals that they are composed of numerous pencil-like ZnO nanorods with a fine nanotip on the bare Si substrate. They are packed in a disordered manner. Highly oriented and dense ZnO hexagonal nanorod arrays with the average diameters of 300 nm lengths of about 1.2 μm are separated from each other on the Cu substrate, as shown in Fig. 2(b). Meanwhile, in the case of the Si substrate coated with ZnO seeds, ZnO nanorod arrays with densely aligned and highly preferential growth occurring along the *c*-axis orientation can also be observed (Fig. 2(c)), with average diameters of 300 nm and lengths of about 1.4 μm. Compared with the Fig. 2(a) and (b), (c) had been oriented much higher, which was consistent with the XRD image. With ZnO seeds, the nucleation density (Fig. 2(c)) was remarkably higher than that of ZnO nanorod arrays grown on without seeds (Fig. 2(a)). Nucleation of ZnO nanorods on ZnO seeds has a lower free energy barrier of activation than that on the bare substrate. So based on the ZnO seeds film at the Si substrate ZnO nanorods formed. Therefore, the ZnO seeds were crucial for the aligned growth.

The study on different substrates' effects of ZnO nanorod arrays growth may lead to an enhanced understanding of the controllable growth of ZnO crystal and nanostructures, which will be useful for the application in novel nanodevices. The oriented growth is important for many applications of nano-/micro-structures. By using the proper substrate and the reaction conditions, the well aligned nanorod arrays can grow on the substrate. It can be explained that the different morphologies of the resultant nanorods should be relied on the substrates, which is an important factor governed by the chemical adsorption and subsequent nucleation and growth [31,32]. At the same time, the SEM image of the products demonstrates that the single-crystal silicon substrate promote the nucleation and the occurrence of anisotropic growth and induces the formation of regular nanostructures. Cu substrate played an important role in inducing the highly oriented ZnO nanorod arrays. Meanwhile, ZnO seeds layer on the substrate may lower the lattice mismatch between the deposition and the substrate and may also lower the free energy barrier of activation. It can help not only to control the nanorod density but also to have a strong impact on the orientation of the nanorod arrays. Generally speaking, the coverage density and orientation of the nanorods would affect the intensity

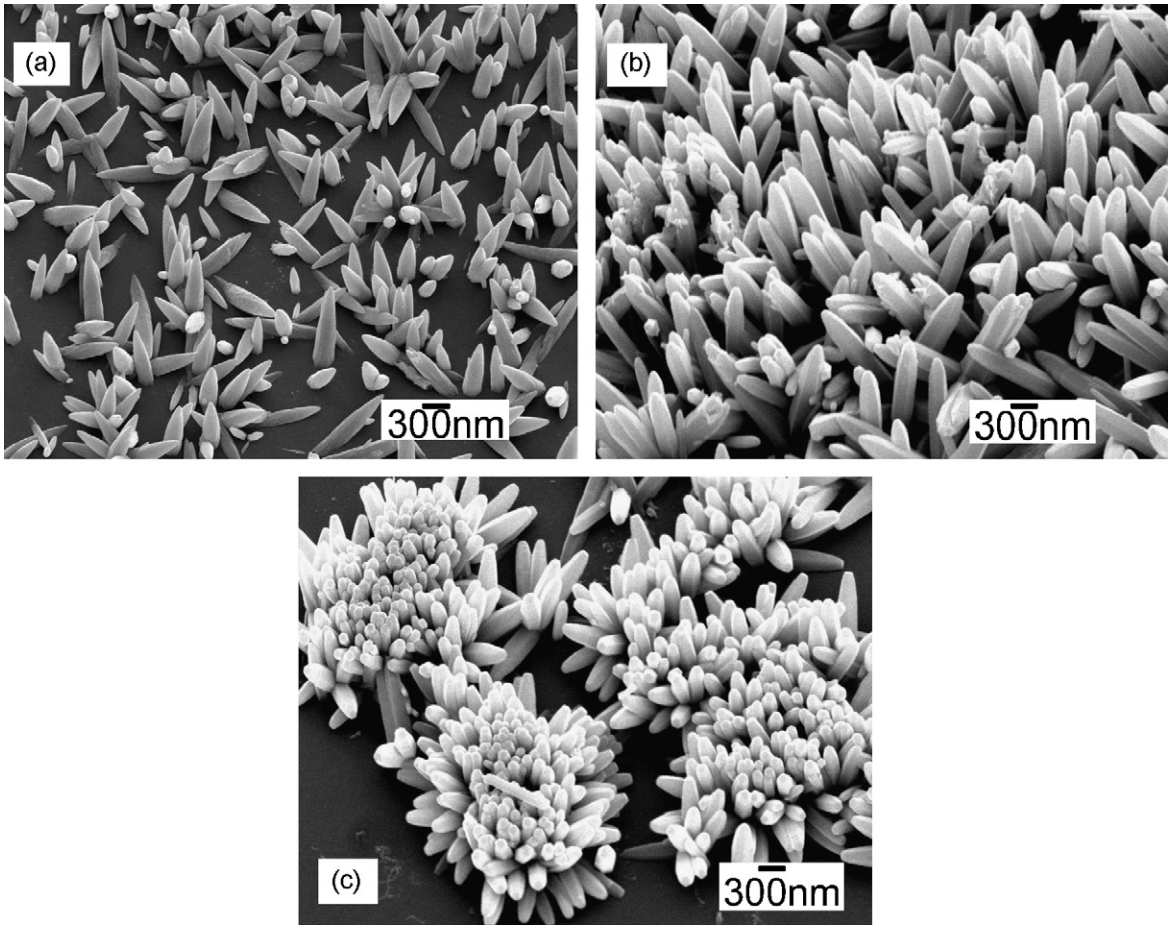

Fig. 2. SEM images of the as-prepared ZnO nanorods with the same condition on a different substrate of the bare Si substrate (a), Cu substrate (b) and Si substrate coated with ZnO seeds (c).

of the XRD diffraction peak, which was in consistent with the XRD images in our experiment.

Photoluminescence (PL) spectroscopy is an effective technique for evaluating the optical properties of semiconductor materials. Fig. 3 shows the typical room-temperature PL spectra of the ZnO nanocrystals fabricated at the same condition on a different substrate. It can be observed that each spectrum consists of a weak band ultraviolet (UV) PL band located at 380 nm. Two weak green emission bands centered at 550 and 570 nm, a strong yellow emission band centered at 600 nm. Generally speaking, the UV emission of ZnO was attributed to an exciton-related activity [33], and the green emission was due to the point defects, such as oxygen vacancies or impurities [34]. The deep level involved in the yellow luminescence was likely interstitial oxygen [35], and perhaps had much to do with the ZnO structure [36]. From Fig. 3(b), it could be seen that the PL peak in the UV intensities has increased a little, and the green and yellow intensities gradually decreased by using the Cu substrate. Moreover, compared with the above two PL curves, the UV emission peak increased greatly again, this indicated potential applications for short-wavelight-emitting photonic devices. The green and yellow light intensities decreased again by using the Si substrate coated with ZnO seeds (Fig. 3(c)). It may be inferred that the sharper peak the UV emission, the more perfect crystallization the samples would have been. From the above, ZnO nanorod arrays fabricated on Si substrate coated with ZnO seeds were optimum for the structure, morphologies and optical properties.

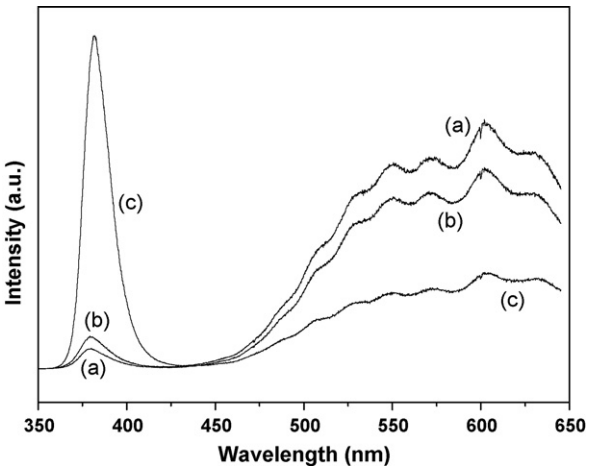

Fig. 3. Room-temperature photoluminescence spectra of ZnO nanorod fabricated with the same condition on a different substrate of the bare Si substrate (a), Cu substrate (b) and Si substrate coated with ZnO seeds(c).

Raman scattering spectrum is very useful and sensitive for determining crystal perfection and structural defects. It is used here to clarify the structure of ZnO nanostructures. Wurtzite-type ZnO belongs to the space group C^4 ($P63mc$) with two formula units in the primitive cell. According to the group theory, single-crystalline ZnO has eight sets of optical phonon modes at Γ point of the Brillouin zone, classified as $A_1 + E_1 + 2E_2$ modes (Raman active), $2B_1$ modes (Raman silent), and $A_1 + E_1$ modes (infrared active). Both A_1 and E_1 modes are polar and split into transverse (TO) and longitudinal

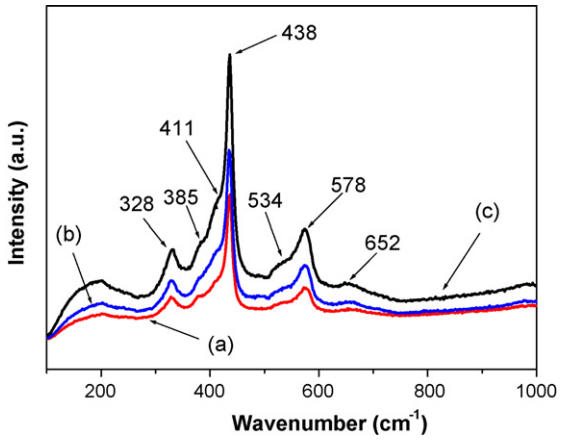

Fig. 4. Raman scattering spectra of the ZnO nanorods prepared by the hydrothermal method with the same condition on a different substrate of a bare Si substrate (a), Cu substrate (b) and Si substrate coated with ZnO seeds (c).

optical (LO) phonons. Nonpolar phonon modes with symmetry E_2 have two frequencies, E_2 (H) is associated with oxygen atoms and E_2 (L) is associated with Zn sublattice. For ZnO single-crystal materials, among the eight sets of optical modes, A_1, E_1, and E_2 are Raman active. Fig. 4 shows the Raman scattering spectra of the ZnO nanorods on different substrates observed at room temperature. Raman shifts of the peaks are assigned to corresponding phonon mode according to Ref. [36], and the phonon modes are labeled. As we can see in the spectra, a sharp, strong and dominant E_2 (H) mode of ZnO located at 438 cm^{-1} is observed, which is the intrinsic characteristic of the Raman active mode of wurtzite hexagonal ZnO [37]. This result is in good agreement with the XRD analysis. Furthermore, E_2 (H) of (c) is much higher than that of (b) and E_2 (H) of (b) is much higher than that of (a), which may be caused due to the different degree of crystallization. The peak at 411 cm^{-1} corresponds to the E_1 (TO) mode, but it is not obvious. As the characteristic peak of hexagonal wurtzite ZnO, the E_2 (high) at 438 cm^{-1} is very intense. The asymmetrical and line-broadening characteristics mask E_1 (TO) on the left-hand side of E_2 (H). The peak at 578 cm^{-1} is attributed to the E_1 (LO) mode, which is caused by the defects such as oxygen vacancy, zinc interstitial, or their complexes and free carriers [38]. From the comparative intensity of E_1 (LO), we think that the crystal perfection of (c) is better than that of (b) and (b) is better than that of (a). In other words, the concentration of defects in (a) is a little higher than that of (b) and (c). In addition, the peaks at 385 and 534 cm^{-1} correspond to A_1 (TO) and A_1 (LO) phonons, respectively. In addition, the peaks at 328 and 652 cm^{-1} are due to multiple phonon scattering processes [39]. In Raman measurement, a large luminescence background can be observed through the whole Raman spectrum, which corresponds to the green wavelength. A green emission band has been observed in the PL spectrum of ZnO by the above-band gap excitation and its luminescence mechanism has been investigated. Vanheusden et al. assigned the visible emission to the recombination of electrons in singlely occupied oxygen vacancies with photoexcited holes in the valence band. Dijken et al. proposed that the emission originated from the recombination between a deeply trapped hole in a VO^{**} center and a shallowly trapped electron [40]. Now, the nature of the green emission still remains controversial. However, it is widely accepted that oxygen vacancies are responsible for the green emission. On the other hand, there are a large number of intrinsic defects existing in ZnO. In particular, because of rods ZnO nanostructures, abundant surface defects will lead to the distribution of surface energy levels forming the surface energy band. The sub-bandgap excitation at 488 nm can induce the excitation of surface states [41]. Therefore, the green emission in PL spectra measurement may be related to surface states.

4. Conclusions

In summary, a simple hydrothermal method was developed to synthesize the pencil-like, well aligned and oriented 1D ZnO nanorods, which grew on three kinds of substrates at low temperature without adding any catalysts or templates. The influence of different substrates on the morphologies and photoluminescence properties of the resultant ZnO nanorod arrays has been investigated. In this article, we can provide a choice to grow ZnO nanorods on other substrates, instead of conventional and expensive sapphire substrate. In addition, the two kinds of nanorods we synthesized may have potential applications in novel devices applications, especially, ZnO nanopencils with a fine nanotip can be used in biosensors and field-emission devices. ZnO nanorod arrays with densely aligned and highly preferential growth on Si substrate coated with ZnO seeds may have a relatively stronger UV emission than that of the other samples. Therefore, ZnO nanorod arrays may have potential applications in short-wavelight-emitting photonic devices. The Raman and PL spectra indicated that the surface defects and oxygen vacancies are responsible for the green emission in our ZnO nanorods. The method can be well controlled, which may make it convenient for the controllable synthesis of other semiconductor nanomaterials.

Acknowledgements

The authors thank the National Natural Science Foundation of China (Grant Nos. 60778040 and 10804036), the Ministry of Science and Technology of China (863) (Item No. 2007AA032400448), the Science and Technology Bureau of Jilin province (Item No. 20060518), gifted youth program of Jilin province (Nos. 20060123 and 20080151) and the Science and Technology Bureau of Key Program for Ministry of Education (Item No. 207025) for financial support.

References

[1] Z.W. Pan, Z.R. Dai, Z.L. Wang, Science 291 (2001) 1947.
[2] Y. Caglar, S. Ilican, M. Caglar, F. Yakuphanoglu, J. Wu, K. Gao, P. Lu, D. Xue, J. Alloys Compd. 481 (2009) 885.
[3] H.C. Cheng, C.F. Chen, C.Y. Tsay, J.P. Leu, J. Alloys Compd. 475 (2009) L46.
[4] S. Musić, A. Šarić, S. Popović, J. Alloys Compd. 448 (2008) 277.
[5] J.T. Hu, T.W. Odom, C.M. Lieber, Acc. Chem. Res. 32 (1999) 435.
[6] L.L. Yang, Q.X. Zhao, M. Willander, J. Alloys Compd. 469 (2009) 623.
[7] Y. Xia, P. Yang, Y. Sun, Y. Wu, B. Mayers, B. Gates, Y. Yin, F. Kim, H. Yan, Adv. Mater. 15 (2003) 373.
[8] R. Yousefi, B. Kamaluddin, J. Alloys Compd. 479 (2009) L11.
[9] F.A. Ponce, D.P. Bour, Nature 386 (1997) 351.
[10] D. Yuan, G.S. Wang, Y. Xiang, Y. Chen, X.Q. Gao, G. Lin, J. Alloys Compd. 478 (2009) 489.
[11] T. Zhang, W. Dong, M. Keeter-Brewer, K. Sanjit, R.N. Njabon, Z.R. Tian, J. Am. Chem. Soc. 128 (2006) 10960.
[12] K. Maeda, T. Takata, M. Hara, N. Saito, Y. Inoue, H. Kobayashi, K. Domen, J. Am. Chem. Soc. 127 (2005) 8286.
[13] M.H. Huang, S. Mao, H. Feick, H. Yan, Y. Wu, H. Kind, E. Weber, R. Russo, P.D. Yang, Science 292 (2001) 1897.
[14] P.X. Gao, Y. Ding, W.J. Mai, W.L. Hughes, C.S. Lao, Z.L. Wang, Science 309 (2005) 1700.
[15] X.H. Sun, S. Lam, T.K. Sham, F. Heigl, A. Jurgensen, N.B. Wong, J. Phys. Chem. B 109 (2005) 3120.
[16] G.Z. Shen, Y. Bando, B.D. Liu, D. Golberg, C. Lee, J. Adv. Funct. Mater. 16 (2006) 410.
[17] S.R. Hejazi, H.R. Madaah Hosseini, M. Sasani Ghamsari, J. Alloys Compd. 455 (2008) 353.
[18] A. Umar, S.H. Kim, J.H. Kim, A. Al-Hajry, Y.B. Hahn, J. Alloys Compd. 463 (2008) 516.
[19] M. Umetsu, M. Mizuta, K. Tsumoto, S. Ohara, S. Takami, H. Watanabe, I. Kumagai, T.A. Dschiri, Adv. Mater. 17 (2005) 2571.
[20] H.D. Yu, Z.P. Zhang, M.Y. Han, X.T. Hao, F.R. Zhu, J. Am. Chem. Soc. 127 (2005) 2378.

[21] F.H. Zhao, W.J. Lin, M.M. Wu, N.S. Xu, X.F. Yang, Z.R. Tian, Q. Su, Inorg. Chem. 45 (2006) 3256.
[22] C.L. Yan, D.F. Xue, L.J. Zou, J. Alloys Compd. 453 (2008) 87.
[23] R. Yi, H.F. Zhou, N. Zhang, G.Z. Qiu, X.H. Liu, J. Alloys Compd. 479 (2009) L50.
[24] J.P. Cheng, Z.M. Liao, D. Shi, F. Liu, X.B. Zhang, J. Alloys Compd. 480 (2009) 741.
[25] J.H. Yang, X.Y. Liu, L.L. Yang, Y.X. Wang, Y.J. Zhang, J.H. Lang, M. Gao, B. Feng, J. Alloys Compd. 477 (2009) 632.
[26] C.D. Lokhande, P.M. Gondkar, S.M. Rajaram, V.R. Shinde, S.-H. Han, J. Alloys Compd. 475 (2009) 304.
[27] J.H. Yang, J.H. Zheng, H.J. Zhai, L.L. Yang, Cryst. Res. Technol. 44 (2009) 87.
[28] P. Tonto, O. Mekasuwandumrong, S. Phatanasri, V. Pavarajarn, P. Praserthdam, Ceramics International 34 (2008) 57.
[29] S.H. Yoon, D.J. Kim, J. Cryst. Growth 303 (2007) 568.
[30] Y. Kajikawa, S. Noda, H. Komiyama, Chem. Vapor Depos. 8 (2002) 99.
[31] J.H. Yang, J.H. Lang, L.L. Yang, et al., J. Alloys Compd. 450 (2008) 521.
[32] L. Vayssieres, Adv. Mater. 15 (2003) 464.
[33] D.M. Bengal, Y.F. Chen, Z. Zhu, T. Yao, Appl. Phys. Lett. 70 (1997) 2230.
[34] B.K. Choi, D.H. Chang, Y.S. Yoon, S.J. Kang, J. Mater. Sci. 10854 (2006) 9036.
[35] D. Li, Y.H. Djurisic, A.B. Leung, Z.T. Liu, M.H. Xie, S.L. Shi, S.J. Xu, W.K. Chan, Appl. Phys. Lett. 85 (2004) 1601.
[36] Y.J. Xing, Z.H. Xi, Z.Q. Xue, X.D. Zhang, J.H. Song, R.M. Wang, J. Xu, Y. Song, S.L. Zhang, D.P. Yu, Appl. Phys. Lett. 83 (2003) 1689.
[37] W.D. Yu, X.M. Li, X.D. Gao, P.S. Qiu, W.X. Cheng, A.L. Ding, Appl. Phys. Lett. 84 (2004) 2658.
[38] F. Decremps, J. Pellicer-Porres, A.M. Saitta, J.C. Chervin, A. Polian, Phys. Rev. B 65 (2002) 92101.
[39] Y.H. Tong, Y.C. Liu, C.H. Shao, Y.X. Liu, C.S. Xu, J.Y. Zhang, Y.M. Lu, D.Z. Shen, X.W. Fan, J. Phys. Chem. B 110 (2006) 14714.
[40] A. van Dijken, E.A. Meulenkamp, D. Vanmaekelbergh, A. Meijerink, J. Phys. Chem. B 104 (2000) 1715.
[41] A. Van Dijken, E.A. Meulenkamp, D. Vanmaekelbergh, A. Meijerink, J. Phys. Chem. B 104 (2000) 1715.